Localization of Multiscale Screened Poisson Equation

Viktor Bäck [*] [†]

June 18, 2012

Abstract

In this paper we investigate a local fine scale problem which arises in various multiscale methods, see e.g. [1]. Local fine scale problems are solved and used to modify coarse scale basis functions. We analyze the decay of these basis functions in the case of localization of the screened Poisson equation, and state a Proposition in which we get a theoretical bound of the decay. Furthermore we present extensive numerical tests which confirms our theoretical results. The screened Poisson equation can be view as a temporal discrete parabolic equation, and can be used to model time-dependent flow in porous media.

[*]Department of Information Technology, Uppsala University, Box 337 SE-751 05 Uppsala, Sweden

[†]Supervisor: Axel Målqvist

1 Introduction

Many problems in science and engineering have solutions with multiscale features. Composite materials can have, for example, thermal, electrical or elastic properties which vary over many different scales. Another important category of multiscale problems is simulation of porous media flow, such as oil reservoir simulation, groundwater flow, storage of carbon dioxide, etc.

In order to resolve fine scale features using a standard one mesh finite element method, a very fine computational grid is necessary. This results in a huge problem which require extensive computational resources. Multiscale methods presents a way to deal with this problem by approximating the over all impact of the fine scale fluctuations on the large scale solution, but without resolving all fine scale features globally. Due to a splitting of the original problem into local independent problems, the multiscale method presented in this paper can be parallelized in a natural way.

Early in the development of multiscale methods, T.J.R. Hughes published a paper [2] where the framework for the variational multiscale method (VMS) was presented. In VMS, the fine part and the coarse part of the solution are decoupled via a course scale residual. The problem is then further decoupled, localized and solved using analytical techniques on the fine scale. A modified coarse scale equation is then obtained, which takes fine scale variations into account. This method was advanced by Larson and Målqvist in [1] where the domain of the localized problems were allowed to grow in size and an adaptive algorithm was implemented. Other similar multiscale methods have also been presented, e.g. the multiscale finite element method [3].

Common for these methods is the lack of convergence analysis for general coefficients. When results do exist (see e.g. [4]), it is under very special assumptions on coefficients (e.g. periodicity). However, in [5] A. Målqvist and D. Peterseim proves that the localized solutions to the Poisson equation (solved in the kernel of a coarse scale interpolant) decays exponentially for general coefficients, and thereby confirms previous numerical indications. This result further motivates the localization of corrector problems (see Section 3.1) for the Poisson equation.

In this paper we apply the method presented in [1] to the screened Poisson equation. In Proposition 2, we state that the error due to localization of corrector problems decay exponentially in the size of the local problem, and note that the proof of this statement follows by small modification of the proof of Lemma 6 in [5].

The paper is outlined in the following way. In Section 2 the screened Poisson

equation, basic notation and an introduction to a standard finite element method is presented. Section 3 introduces the multiscale method used throughout the paper. In Section 4 error analysis is performed and the main result, Proposition 2, is stated in more detail.

2 Background

2.1 Preliminaries

The problem we consider is the screened Poisson equation with zero Dirichlet boundary conditions. This equation is given by

$$-\nabla \cdot A\nabla u + \epsilon^{-2}u = f, \quad \text{in } \Omega, \tag{2.1}$$

$$u = 0, \quad \text{on } \partial\Omega, \tag{2.2}$$

where $A \in L^\infty(\Omega)$ with $0 < \alpha \leq A \leq \beta$, $f \in L^2(\Omega)$, $0 < \epsilon \in \mathbb{R}$, and Ω is a polygonal domain in $\mathbb{R}^d, d = 1, 2, 3$. The corresponding variational formulation reads: find $u \in V = \{v \in H^1(\Omega) : v|_{\partial\Omega} = 0\}$ such that

$$a(u, v) := (A\nabla u, \nabla v) + \epsilon^{-2}(u, v) = (f, v) =: F(v), \quad \forall v \in V, \tag{2.3}$$

where

$$(u, v) := \int_\Omega u \cdot v \, dx \tag{2.4}$$

is the standard L^2-inner product. The bilinear form $a(\cdot, \cdot)$ induces the norm

$$|||\cdot|||^2 := |||\cdot|||_\Omega^2 := \|A^{1/2}\nabla \cdot \|^2_{L^2(\Omega)} + \epsilon^{-2}\| \cdot \|^2_{L^2(\Omega)}. \tag{2.5}$$

We adopt the following notation. Let $\mathcal{T}_H$ be a triangulation of Ω, where H is an upper bound of the diameter of triangles in $\mathcal{T}_H$, and let $\mathcal{N}$ be the set of all interior nodes in the triangulation. The notation $\delta := \epsilon/H$ will be frequently used. Next, define the finite element space $V_H = \{v \in V \cap C^0(\Omega) : v|_T \text{ is linear } \forall T \in \mathcal{T}_H\} \subset V$. Also, introduce a tent function for each node $x \in \mathcal{N}$, i.e. a continuous piecewise linear function function

$$\lambda_x(y) = \begin{cases} 1 & \text{if } y = x \\ 0 & \text{if } y \in \mathcal{N} \setminus \{x\}. \end{cases} \tag{2.6}$$

These tent functions form a basis in $V_H = \text{span}\{\lambda_x : x \in \mathcal{N}\} \subset V$.

Remark 1 *Temporal discretization of the heat equation using the backward Euler scheme results in*

$$\frac{u^n - u^{n-1}}{k} - \nabla \cdot A\nabla u^n = g \tag{2.7}$$

$$\implies \quad \frac{u^n}{k} - \nabla \cdot A\nabla u^n = g + \frac{u^{n-1}}{k} =: f, \tag{2.8}$$

where u^n is the solution at time step n and k is the length of the time step. Thus (2.1) *can be viewed as a temporal discrete heat equation with time step ϵ^2.*

2.2 Finite element method

In this subsection we briefly introduce a standard finite element method and discuss some of its limitations.

We reformulate the original problem (2.1) using weak derivatives, and consider the weak form

$$a(u, v) = F(v), \quad \forall v \in V. \tag{2.9}$$

The variational formulation (2.9) has a unique solution $u \in V$ according to the Lax-Milgram theorem, provided that $a(\cdot, \cdot)$ is coercive and bounded. We then seek to approximate u by $u_H \in V_H$, where

$$a(u_H, v) = F(v), \quad \forall v \in V_H. \tag{2.10}$$

As in the case of the variational formulation, boundedness and coercivity of $a(\cdot, \cdot)$ imply existence and uniqueness of u_H. The fact that u_H is the best approximation in V_H of u (with respect to $|||\cdot|||$) is a consequence of Galerkin orthogonality, which sates that

$$a(u - u_H, v) = 0, \quad \forall v \in V_H. \tag{2.11}$$

Thus the error $u - u_H$ is orthogonal to all $v \in V_H$ with respect to $a(\cdot, \cdot)$.

Recall that a basis of V_H is obtained by introducing tent-functions λ_x for each node $x \in \mathcal{N}$, i.e. $V_H = \text{span}\{\lambda_x : x \in \mathcal{N}\}$. Thus $u_H = \sum_{x\in\mathcal{N}} c_x\lambda_x$ for some coefficients $c_x \in \mathbb{R}$. Solving (2.10) for each $v \in V_H$ is equivalent to solving (2.10) for each basis function $\lambda_y, y \in \mathcal{N}$. Thus (2.10) can be reduced to

$$a\left(\sum_{x\in\mathcal{N}} c_x\lambda_x, \lambda_y\right) = F(\lambda_y), \quad \forall y \in \mathcal{N}, \tag{2.12}$$

which is a sparse linear system of equations that can be solved analytically or numerically.

Assuming Ω to be convex and $A \in C^1(\Omega)$, the error estimate

$$|||u - u_H||| < C(A, f, \alpha)H \tag{2.13}$$

holds with a constant C that depends on A, f and α. In particular if A is periodic, e.g. $A = A(x/\epsilon)$, then

$$|||u - u_H||| \lesssim \frac{H}{\epsilon}. \tag{2.14}$$

Thus it is required that $H \lesssim \epsilon$ in order to obtain a reliable solution using the method (2.10), which results in a huge problem when solving (2.12) if ϵ is small. Multiscale methods presents a solution to this issue, and in the next section one such method is introduced.

3 Multiscale method

3.1 Modified coarse problem

We proceed by defining the fine scale space, which can be done in different ways. Let $V^f = \{v \in V : \mathcal{I}_H v = 0\}$ represent fine scale features, where $\mathcal{I}_H : V \to V_H$ is an inclusion operator specified below. For $v \in V_H$ define $Tv \in V^f$ such that

$$a(Tv, w) = -a(v, w), \quad \forall w \in V^f. \tag{3.1}$$

Thus $T : V_H \to V^f$. The existence and uniqueness of Tv is assured by the Lax-Milgram theorem (note that $a(\cdot, \cdot)$ is coercive and bounded). From (3.1) it is clear that $Tv + v$ is a-orthogonal to w, for all $w \in V^f$. This leads to the orthogonal splitting

$$V = V_H^{ms} \oplus V^f, \tag{3.2}$$

where $V_H^{ms} = \text{span}\{v + Tv : v \in V_H\}$. Thus, a solution u to (2.3) can be written as $u = u_H^{ms} + u^f$, where $u_H^{ms} \in V_H^{ms}$ and $u^f \in V^f$. Note that a basis in V_H^{ms} is obtained by solving (3.1) for each coarse basis function λ_x, i.e. for each $x \in \mathcal{N}$ solve

$$a(\phi_x, v) = -a(\lambda_x, v), \quad \forall v \in V^f, \tag{3.3}$$

where $\phi_x := T\lambda_x$. Then $V_H^{ms} = \text{span}\{\lambda_x + \phi_x : x \in \mathcal{N}\}$.

Since there is a one-to-one correspondence between $\{\lambda_x\}_{x\in\mathcal{N}}$ and $\{\phi_x\}_{x\in\mathcal{N}}$, $\{\lambda_x + \phi_x\}_{x\in\mathcal{N}}$ can be viewed as a modified coarse scale basis which also contain fine scale

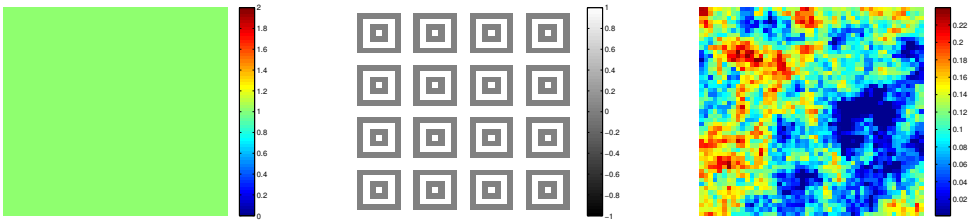

Figure 3.1: Coefficient A_1 (left), A_2 (middle), A_3 (right)

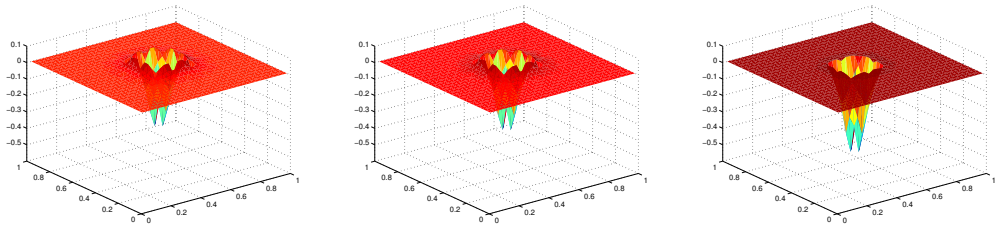

Figure 3.2: Solution ϕ_x of (3.3) with coefficient $A_1 = 1$ and $\delta = 10$ (left), $\delta = 1$ (middle), $\delta = 0.1$ (right).

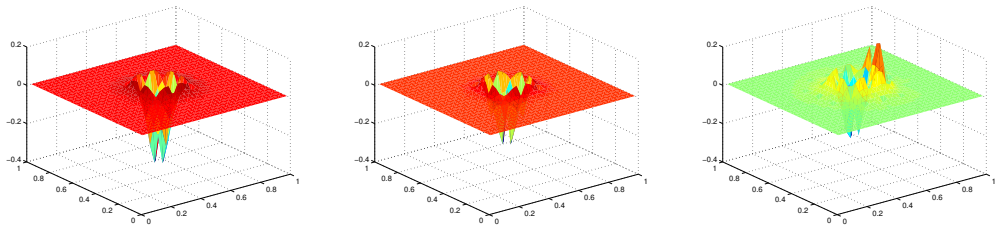

Figure 3.3: Solution ϕ_x of (3.3) with $\delta = 1$ and coefficient $A_1 = 1$ (left), A_2 discontinuous and periodic (middle. See Figure 3.1), A_3 discontinuous with nodal values from a model of an oil reservoir (right. See Figure 3.1.)

information. In Figure 3.2, 3.3 typical fine scale solutions of (3.3) are depicted, using different A and $\delta = \epsilon/H$.

In [5] this modified basis is used to obtain the modified coarse problem: find $u_H^{ms} \in V_H^{ms}$ such that

$$a(u_H^{ms}, v) = F(v), \quad \forall v \in V_H^{ms}. \tag{3.4}$$

One problem with the method (3.4) is that ϕ_x in general have global support in Ω, which results in a large problem when solving (3.3) for each coarse basis function λ_x. We will now discuss a way to localize the corrector problem (3.3).

3.2 Localization

Consider the problem of solving (3.3) given a node $x \in \mathcal{N}$. For $k \in \mathbb{N}$, define the k-th order patch (or a patch with k layers) $\omega_{x,k} \subset \Omega$ recursively as

$$\omega_{x,1} = \bigcup_{\{T \in \mathcal{T}_H : x \in \bar{T}\}} T, \tag{3.5}$$

$$\omega_{x,k} = \bigcup_{\{T \in \mathcal{T}_H : \bar{T} \cap \bar{\omega}_{x,k-1} \neq \emptyset\}} T. \tag{3.6}$$

Figure 3.4 illustrates a patch with 1 layer, and a patch with 2 layers. Introduce the localized fine scale space $V^f(\omega_{x,k}) := V^f \cap H_0^1(\omega_{x,k})$. As will be demonstrated in Section 5, the decay of ϕ_x away from x is very rapid (exponential). This allows for an approximation of ϕ_x by means of restricting the fine scale space V^f to the smaller space $V^f(\omega_{x,k})$ when solving (3.3), i.e. find $\phi_{x,k} \in V^f(\omega_{x,k})$ such that

$$a(\phi_{x,k}, v) = -a(\lambda_x, v), \quad \forall v \in V^f(\omega_{x,k}). \tag{3.7}$$

An approximation of ϕ_x is obtained by extending $\phi_{x,k}$ to zero on $\Omega \setminus \omega_{x,k}$, and a localized version of V_H^{ms} is obtained as $V_{H,k}^{ms} = \text{span}\{\lambda_x + \phi_{x,k} : x \in \mathcal{N}\}$.

We can now formulate an approximation of (3.4): find $u_{H,k}^{ms} \in V_{H,k}^{ms}$ such that

$$a(u_{H,k}^{ms}, v) = F(v), \quad \forall v \in V_{H,k}^{ms}. \tag{3.8}$$

4 Error analysis

The following Proposition provides an upper bound of the error due to localization of problem (3.3).

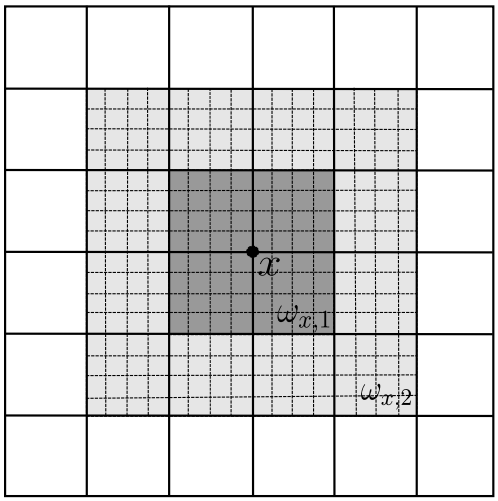

Figure 3.4: A patch with 1 layer (dark gray region), and a patch with 2 layers (dark gray region plus light gray region).

Proposition 2 (Generalization of Lemma 6 in [5]) *For $x \in \mathcal{N}, k, l \geq 2 \in \mathbb{N}, \delta = \epsilon/H$ and $\mathcal{I}_H$ as the Clément Interpolant (as presented in [5]), the estimate*

$$\left|\left|\left|\phi_x - \phi_{x,kl}\right|\right|\right| \lesssim C_2 \left(\frac{C_1 \min(1,\delta)}{l}\right)^{\frac{k-2}{2}} |||\phi_x|||_{\omega_{x,l}} \tag{4.1}$$

holds with constants C_1, C_2 that only depend on the shape regularity parameter ρ of the finite element mesh $\mathcal{T}_H$, but not on $x, k, l,$ or H.

Remark 3 *We note that the proof of Lemma 6 in [5] with small modification holds for the modified bilinear form $a(u,v) = (A^{1/2}\nabla u, \nabla v) + \epsilon^{-2}(u,v)$. The key result in [5], $\|\phi_x\|_{L^2(\Omega)} \lesssim H\|A^{1/2}\nabla\phi_x\|_{L^2(\Omega)}$, can be improved in the setting of the current paper. Since $\|\phi_x\|_{L^2(\Omega)} \leq \epsilon\left(\|A^{1/2}\nabla\phi_x\|^2 + \epsilon^{-2}\|\phi_x\|^2\right)^{1/2}$ and $\|\phi_x\|_{L^2(\Omega)} = \|\phi_x - \mathcal{I}_H\phi_x\|_{L^2(\Omega)} \lesssim H\,|||\phi_x|||_{L^2(\Omega)}$ we conclude*

$$\|\phi_x\|_{L^2(\Omega)} \lesssim \min(H,\epsilon)\,|||\phi_x|||_{L^2(\Omega)} = H\min(1,\delta)\,|||\phi_x|||_{L^2(\Omega)}\,. \tag{4.2}$$

In Figure 4.1 the error $\phi_x - \phi_{x,k}$ is depicted in different cases of the coefficient A. Note that the largest error occurs on the boundary of the patch $\omega_{x,k}$ on which $\phi_{x,k}$ is calculated.

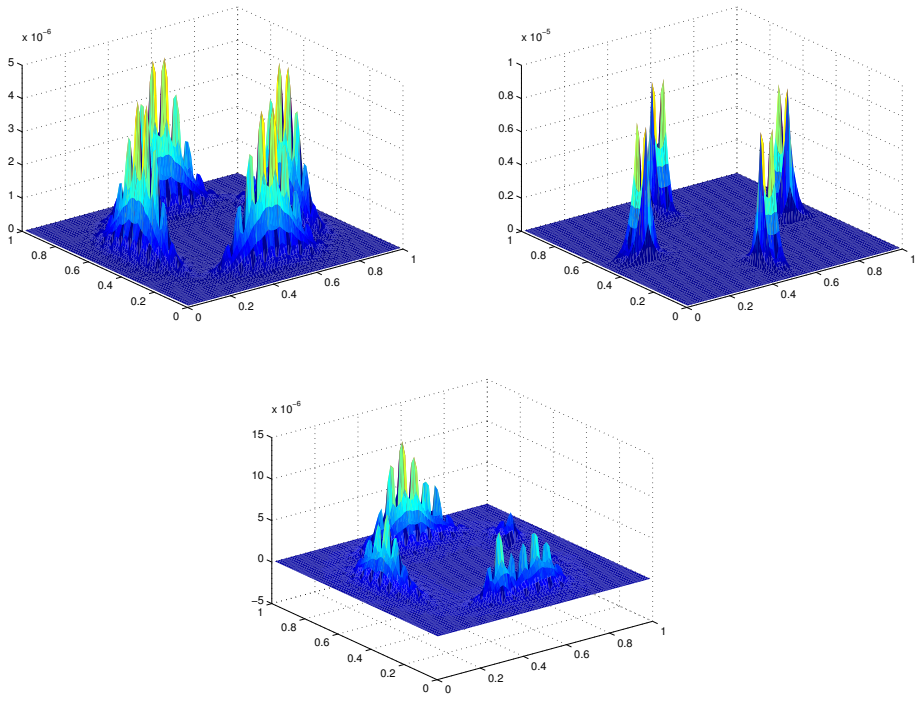

Figure 4.1: Images of $\phi_x - \phi_{x,k}$ for $A_1 = 1$ (top left), A_2 discontinuous and periodic (top right. See Figure 3.1), A_3 discontinuous with nodal values from a model of an oil reservoir (bottom. See Figure 3.1).

5 Numerical results

Numerical results verifying Proposition 2 now follows.

Observe that (4.1) can be written

$$Q := \frac{|||\phi_x - \phi_{x,kl}|||}{|||\phi_x|||_{\omega_{x,l}}} \lesssim C_2 \left(\frac{C_1 \min(1, \delta)}{l} \right)^{\frac{k-2}{2}}. \tag{5.1}$$

The quotient Q is calculated on a cartesian grid with mesh size $h = 0.025$ on $\Omega = [0, 1] \times [0, 1]$ for different parameter values. We let $\mathcal{I}_H$ be the nodal interpolant and consider three different choices of A; A_1, A_2 and A_3 (see Figure 3.1). The Coefficient A_1 is constant with value one. The coefficient A_2 is periodic and discontinuous with value 1 on bright regions and value 0.01 on dark regions. The

thickness of the dark lines are 0.0286, the box-like pattern is repeating with period 0.257, the contrast $\alpha/\beta = 10^2$. The coefficient A_3 is discontinuous with nodal values taken from a model of an oil reservoir and with contrast $\alpha/\beta = 10^5$. In Figure 5.1 Q is plotted against different values of $\delta = \epsilon/H$. The asymptotical behavior of Q as δ grows larger is clear, and reflects the fact that (2.1) transitions into an elliptic equation which does not depend on ϵ. Also, the value of Q starts to drop drastically when δ is of the same order of magnitude as predicted by (4.1).

Next, consider varying k when calculating Q, keeping δ fixed (see Figure 5.2). The exponential decay of Q in k is evident, which agrees well with (5.1).

6 Conclusions

As noted in Remark 1, the screened Poisson equation (2.1) can be seen as a temporal discrete parabolic equation with time step ϵ^2. Proposition 2 (whose proof should impose no difficulty) reveals that the decay of basis functions given by (3.3) is more rapid if δ is of order 1 or smaller. This means that the localized problem (3.8) can be solved on smaller patches if δ is decreased, which reduces the computational effort in each time step. It is also worth noting that the set of modified basis functions obtained by solving (3.7) can be reused each time step if the coefficient A is not time-dependent and the same time step is used. Thus it is a matter of optimization when choosing the size of the patches, the time step ϵ, and the mesh size H.

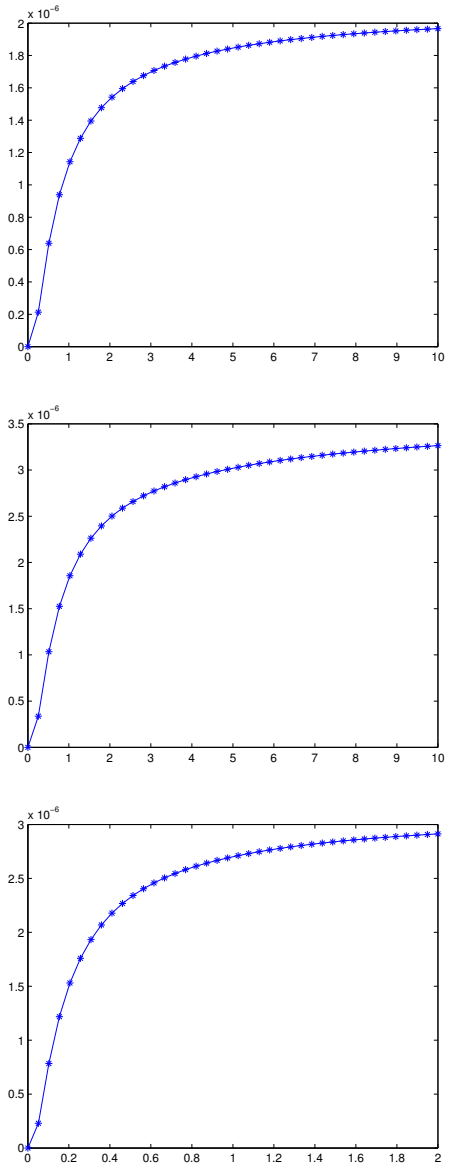

Figure 5.1: Q plotted against δ for $A = A_1$ (top), $A = A_2$ (middle), $A = A_3$ (bottom).

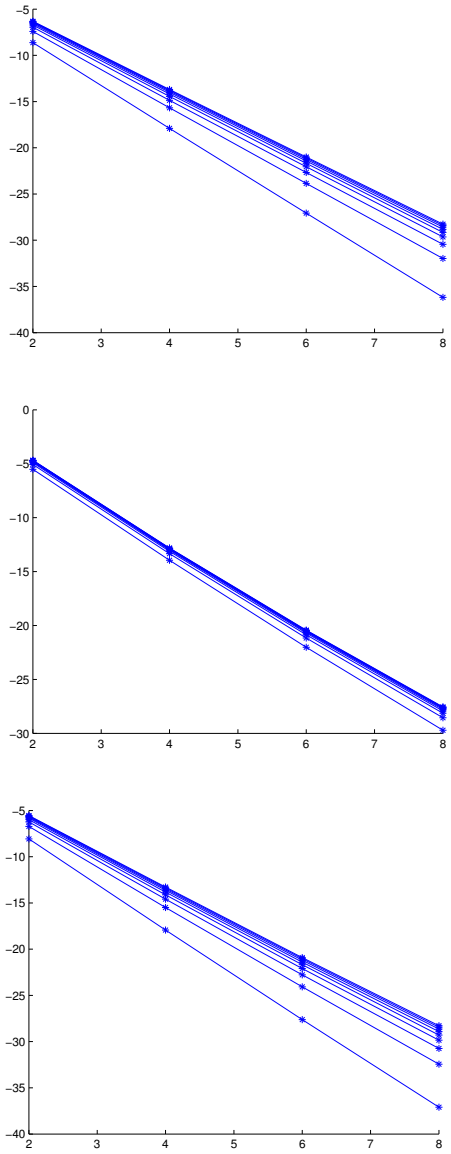

Figure 5.2: $\log Q$ plotted against k for 10 equally distributed values of δ ranging from 1 to 0.001 for $A = A_1$ (top), $A = A_2$ (middle), $A = A_3$ (bottom). Each line corresponds to a value of δ and the slope of the lines increases with δ (e.g. the uppermost line corresponds to $\delta = 1$, the lowermost line corresponds to $\delta = 0.001$).

References

[1] M. G. Larson, A. Målqvist. Adaptive variational multiscale methods based on a posteriori error estimation: energy norm estimates for elliptic problems. *Comput. Methods Appl. Mech. Engrg., 196 (2007):2313–2324.*

[2] T.J.R. Hughes. Multiscale phenomena: Green's functions, the Dirichlet-to-Neumann formulation, subgrid scale models, bubbles and the origins of stabilized methods, *Comput. Methods Appl. Mech Engrg 127 (1995):387–401.*

[3] T.Y. Hou, X.-H. Wu. A multiscale finite element method for elliptic problems in composite materials and porous media, *J. Comput. Phys. 134 (1997):169–189.*

[4] T.Y. Hou, X.-H. Wu, Z. Cai. Convergence of a multiscale finite element method for elliptic problems with rapidly oscillating coefficients, *Math. Comput. 68 (1999):913–943.*

[5] A. Målqvist, D. Peterseim. Localization of elliptic multiscale problems. *arXiv:1110.0692v3.*